J Mater Sci (2011) 46:4630–4637
DOI 10.1007/s10853-011-5365-3

Electrocatalytic evolution of hydrogen on the NiCu/Al_2O_3/nano-carbon network composite electrode

Xuhui Zhao · Masayoshi Fuji · Takashi Shirai · Hideo Watanabe · Minoru Takahashi · Yu Zuo

Received: 15 October 2010 / Accepted: 1 February 2011 / Published online: 11 February 2011

Abstract We present a way to fabricate the NiCu/Al_2O_3/nano-carbon network (NCN) composite electrode by coelectrodepositing NiCu particles, using a novel conductive alumina/NCN composite material as the support. The morphology, crystalline phases, and compositions are characterized by field-emission scanning electron microscope, energy dispersive X-ray spectroscope, X-ray diffraction, and Raman spectroscopy. The electrocatalytic behaviors of this NiCu/Al_2O_3/NCN composite material for hydrogen evolution reaction (HER) in alkaline solution are studied by cathodic polarization curves, electrochemical impedance spectroscopy (EIS), and chronoamperometry. The results show that nickel–copper particles are briefly deposited and uniformly distributed over the carbon layer of the conductive ceramics between alumina grains, in the form of a NiCu solid solution with face-centered cubic structure. The NiCu/Al_2O_3/NCN composite displays a high electrochemical stability in alkaline solution and relatively high electrocatalytic activity for HER due to its relatively high real surface area and high intrinsic electrocatalytic effect of NiCu alloy particles. The associated kinetic parameters of HER are systematically investigated using EIS.

X. Zhao · M. Fuji (✉) · T. Shirai · H. Watanabe · M. Takahashi
Ceramics Research Laboratory,
Nagoya Institute of Technology,
Hommachi 3-101-1, Tajimi, Gifu 507-0033, Japan
e-mail: fuji@nitech.ac.jp

X. Zhao · Y. Zuo
School of Materials Science and Engineering,
Beijing University of Chemical Technology,
Beijing 100029, China

Introduction

Hydrogen is considered as one of the most potential energy carriers because it is clean, efficient, and renewable [1].Water electrolysis is an important technique for production of hydrogen, especially in large quantity production of high purity hydrogen, although it is not the cheapest method of hydrogen production [2, 3]. The main problem with electrolytic hydrogen, which restrains its application at the present, is the high cost and high energy consumption mainly caused by the over-potential of hydrogen evolution reaction (HER) [4, 5]. In order to reduce the over-potential of the electrode reaction, expensive noble metals (such as Pt, Pd) can be considered as electrodes for HER. However, these noble metals are not only high in cost but also limited in resource. Therefore, to decrease the cost and energy consumption of electrolytic hydrogen, it is urgent to find and develop cheap and abundant electrode materials with high electro-catalytic activity for the HER. In general, there are two ways to lower the HER over-potential: (a) increasing an actual intrinsic electrocatalytic effect of the materials by synergistic combination of electrocatalytic components, (b) increasing a large active surface area per unit volume ratio. So, many non-noble metal-based electrode materials are developed by varying surface morphology (high surface roughness) or alloying or compositing, to enhance the electro-catalytic activity for HER [5–17]. However, for low-cost industrial application, the nickel-based materials have long been recognized as most potential electrode materials due to its relatively high activity and low cost [18–20].

This study discusses the results on the use of a novel conductive alumina/nano-carbon network (NCN) composite material as a support for the construction of NiCu/Al_2O_3/NCN composite catalyst for hydrogen evolution.

It is well known that nickel is an active metal for HER. As previously mentioned, nickel can be used as a catalyst due to its high catalytic activity and low cost. The study of alloy electrodes is motivated primarily from the anticipation of a synergistic electrocatalytic benefit from the combined properties of the component metals of alloys. Although copper is not a very active metal for the HER, Solmaz et al. [5, 21] investigated that NiCu alloy electrode in their studies of HER in alkaline medium and found that Ni and Cu had synergistic effect for hydrogen evolution and modification of nickel by copper enhanced its electrocatalytic activity in electrocatalytic evolution of hydrogen. Moreover, one promising characteristic of such alloy electrodes is the good corrosion resistance in the alkaline media. Therefore, NiCu were chosen as catalytic particles in our study. The novel conductive alumina/NCN composite can be considered as a support because of its unique physical and chemical properties. The conductive alumina/NCN composite is fabricated using a novel process by the combination of gel casting and reduction sintering in an inert atmosphere [20, 22]. In this material, inner-connected alumina grains with a content of higher than 99% supply not only high mechanical strength but also physical and thermal stability, and NCNs formed between the grain boundaries of the alumina give electrical conductivity [22, 23]. Moreover, kinds of particle can be deposited onto the carbon networks as introduced in many literatures [24]. Besides, the conductive alumina/NCN composite material has strong electrochemical durability at the high applied potential in both acidic and alkaline environments [25].

In this study, the NiCu/Al_2O_3/NCN composite electrode was prepared by coelectrodepositing nickel and copper on the surface of the conductive alumina/NCN composite. The surface morphology, microstructure, and composition of the NiCu/Al_2O_3/NCN composite electrode material were then analyzed using scanning electron microscopy (SEM), energy dispersive X-ray spectroscope (EDS), and X-ray diffraction (XRD) techniques. The electrocatalytic activities for HER were examined in 1 M NaOH solution by electrochemical methods.

Experimental

Fabrication of NiCu/Al_2O_3/NCN composite electrode

The novel electrically conductive alumina/NCN composite materials was prepared using gel casting and reductive sintering under inert atmosphere (Ar) as introduced in references [22, 23]. The mixture of premix solution contained methacrylamide, corresponding crosslinking agent N,N′-methylenebisacrylamide, alumina powder, and ammonium polycarboxylate acid. The alumina powder of mean particle diameter 0.50 μm (AL 160SG-4, Showa Denko Co., Tokyo, Japan) with solid loading of 80 mass% was used as the resource of the ceramics matrix. Methacrylamide and N,N′-methylenebisacrylamide was dissolved in distilled water as gellants. The alumina powder was dispersed to the solvent with a dispersant, ammonium polycarboxylate acid (Selna D-305, Chukyo Yushi, Nagoya, Japan), by ball milling for 24 h. The well-dispersed slurry was agitated under a vacuum condition for 15 min. Then, ammonium peroxodisulfate as initiator and N,N,N′,N′,-tetramethylethylenediamine as catalyst were added into the slurry to initiate a polymerization reaction and to form gel-green body. The well-dried green body was sintered at 1700 °C for 2 h in a gas-tight furnace (IK-3, Ito Keisoku Co. Ltd, Japan) under argon atmosphere. The surface micrograph of the conductive alumina/NCN composite materials is shown in Fig. 1. In our previous studies [22], the pyrolyzed carbon with a content of about 0.8 wt% in the composite was confirmed to exist in continuous and interconnected carbon networks along the alumina grains through the reduction sintering, which was responsible for the electrical conductivity of the resulted ceramics. For further investigation, the as-prepared composite was cut into small plates (10 × 25 × 2 mm).

The NiCu/Al_2O_3/NCN composite electrode was prepared by coelectrodepositing nickel and copper particles onto the surface of the conductive alumina/NCN composite. Before electrodeposition, the conductive alumina/NCN composite was mechanically polished using sandpapers of various grades, and then washed with distilled water, degreased by ultrasonication in ethanol bath and dried at 90 °C. The coelectrodeposition of nickel and copper particles was performed using a Potentiostat/Galvanostat (HZ-5000, Hokuto Denko Co., Tokyo, Japan) with a

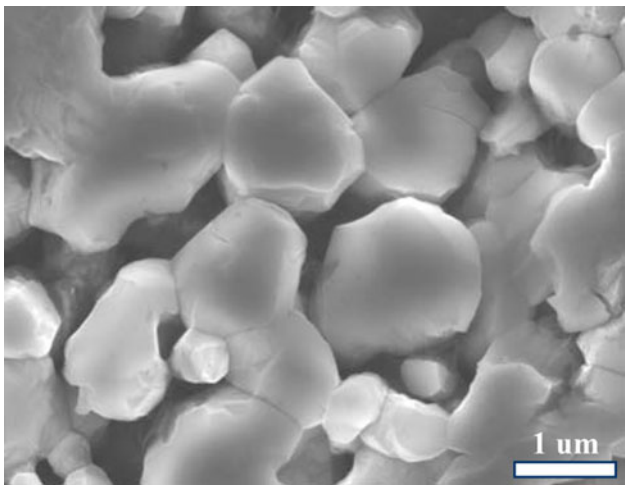

Fig. 1 FE-SEM micrograph of conductive alumina/NCN composite electrode

three-electrode configuration. A platinum sheet was used as the counter electrode (CE) and Ag/AgCl-saturated KCl electrode was used as the reference electrode (RE), respectively. The conductive alumina/NCN composite (Al_2O_3/NCN) electrode was used as working electrode (WE). The WE was covered with an insulated tape, one side leaving an area of about 1 cm^2 exposed to the electrolyte. In order to assure the uniformity of deposit, WE was placed parallel to the CE in the bath and electrolyte was stirred with magnetic stirrer during electrodeposition. The bath composition was 0.53 M $NiSO_4 \cdot 6H_2O$, 0.17 M $Ni(AC)_2 \cdot 4H_2O$, 0.05 M $CuSO_4 \cdot 5H_2O$, 0.26 M $Na_3C_6H_5O_7 \cdot 2H_2O$, and 0.15 M $(NH_4)_2SO_4$. The pH value of the bath was adjusted to 7–8 by using $NH_3 \cdot H_2O$. The bath temperature was kept at ambient temperature (about 20 °C). The electro-deposition conditions were set as a constant potential of −1300 mV (vs. Ag/AgCl-saturated KCl) for 10 s. After electrodeposition, the prepared NiCu/Al_2O_3/NCN composite electrode was rinsed with distilled water and dried.

Characterization for NiCu/Al_2O_3/NCN composite electrode

The morphology and chemical composition of the NiCu/Al_2O_3/NCN composites were examined by field-emission scanning electron microscope (FE-SEM, JSM-7000F, JEOL Ltd., Tokyo, Japan) equipped with EDS. The structural investigation was conducted by the XRD (XRD, RINT, Rigaku Co., Tokyo, Japan) and Raman spectroscopy (NRS-3100, Jasco Co., Tokyo, Japan). NiCu particles are mainly distributed on the carbon surface, and the amounts of NiCu particles are low due to low carbon content of the substrate, which are not detected by XRD. For XRD analysis, the NiCu/Al_2O_3/NCN electrode was prepared under electrodeposition time of 300 s to obtain sufficient NiCu particles.

Electrochemical measurements were carried out by using a potentiostat/galvanostat (HZ-5000, Hokuto Denko Co., Tokyo, Japan) equipped with a FRA5022 frequency response analyzer. A conventional three-electrode cell was used for the electrochemical measurements. The NiCu/Al_2O_3/NCN composite electrode was used as WE, a platinum sheet was used as the CE and an Ag/AgCl-saturated KCl electrode (0.199 mV vs. SHE) was used as RE, respectively. In this study, unless otherwise noted, all voltages were reported with respect to the Ag/AgCl, saturated KCl electrode. The size of the working area exposed to testing solutions was about 1 cm^2. All the electrochemical tests were performed in 1 M NaOH aqueous solutions with N_2 purging before each experiment at ambient temperature and were repeated at least three times. Cathodic polarization measurements were performed in the potential range from −0.8 to −1.8 V at a scan rate of 2 mVs^{-1}. The current densities presented in this study were taken on the basis of the geometric area of the electrodes. Electrochemical impedance spectroscopy (EIS) experiments were conducted in the frequency range of 100 kHZ–10 mHz under different electrode potentials with a 5 mV AC perturbation. The measured value of the reversible electrode potential for the HER in 1 M NaOH was about −950 mV at 293 K with respect to Ag/AgCl, saturated KCl RE [26, 27]. In order to correct the polarization data for IR drop effects, the uncompensated solution resistance values were calculated using the data acquired from the EIS measurements. All the electrochemical tests were performed in 1 M NaOH solutions at ambient temperature and were repeated at least three times. Furthermore, the electrochemical behavior of the prepared electrode for HER was compared to conductive alumina/NCN and graphite (KGR-3, Akechi Ceramics Co. Ltd., Gifu, Japan) electrodes.

Results and discussion

Characterization of the NiCu/Al_2O_3/NCN composite electrode

The surface morphology of the fabricated composite materials was studied using SEM. Figure 2 showed the SEM image and the EDS surface compositional mapping of the NiCu/Al_2O_3/NCN composite electrode. Compared with the surface micrograph of the conductive alumina/NCN composite without depositing Ni–Cu particles (shown in Fig. 1), it can be seen that Ni–Cu particles were mainly electrodeposited and relatively uniformly distributed over the carbon layer of conductive ceramics between alumina grains. The relative contents of the nickel and copper elements on the composite electrode surface were 2.19 and 2.05 atom%, respectively, and the atom ratio of Ni/Cu was about 1:1, determined by EDS analysis. The amount of deposited NiCu particles was roughly estimated by the amount of electricity during the deposition and the contents were about 0.05 mg cm^{-2}.

The fabricated composite electrode materials were examined by XRD to identify the composition and corresponding crystalline structure of the electrode materials. The XRD patterns of the conductive alumina/NCN composite and NiCu/Al_2O_3/NCN composite materials are shown in Fig. 3. In Fig. 3a, a very faint broader diffraction peak at about 10–20° reflected the pyrolyzed nano-size carbon which existed in the interstices and voids in the sintered alumina [27], while other peaks in this diffraction spectrum reflected a crystalline alumina phase in ceramics matrix. But in Fig. 3b, the observed peaks at about 44°, 51°, and 75.5° were relatively obvious for the NiCu/Al_2O_3/

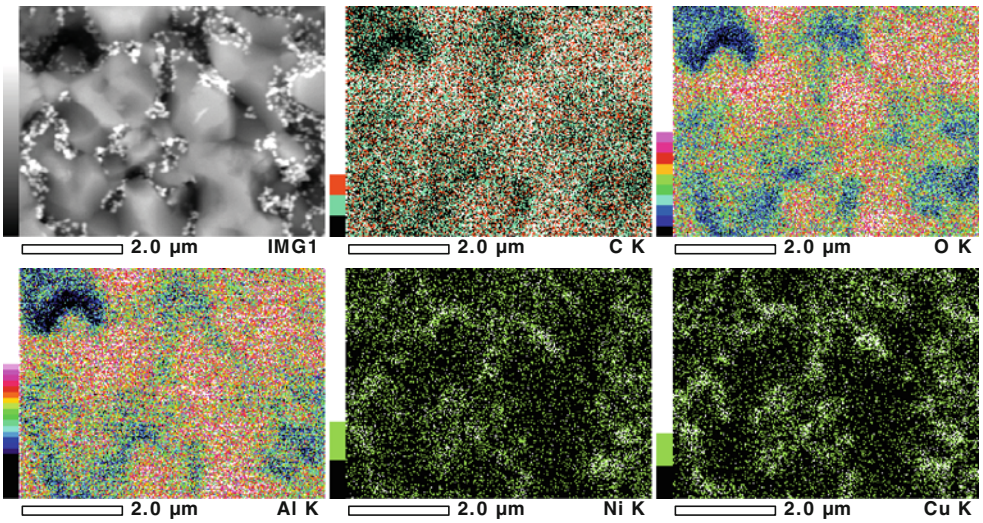

Fig. 2 FE-SEM micrograph and the EDS surface compositional mapping of $NiCu/Al_2O_3/NCN$ composite electrode

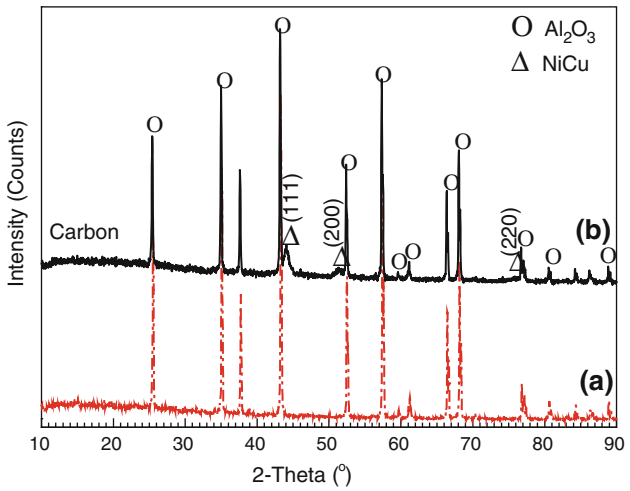

Fig. 3 XRD patterns of (*a*) alumina/NCN and (*b*) $NiCu/Al_2O_3/NCN$ composite electrodes

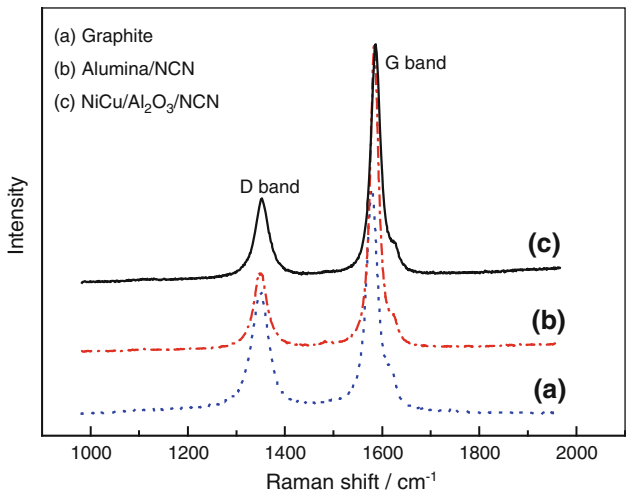

Fig. 4 Raman spectra of (*a*) graphite, (*b*) alumina/NCN, and (*c*) $NiCu/Al_2O_3/NCN$ electrodes

NCN composite as compared with that of the conductive alumina/NCN composite electrode in Fig. 3a. Obviously, these peaks should be related to the electrodeposited Ni–Cu particles. Also, it seemed that electrodeposited particles had face-centered cubic (fcc) structure oriented in (111), (200), and (220) directions, and formed a solid solution based on only the fcc phase [28, 29]. By means of Vegard's law, the calculated Ni and Cu contents in NiCu deposits were about 58 atom% Ni and 42 atom% Cu, consistent with the EDS results. The existence of the carbon with the graphic crystal structure in $NiCu/Al_2O_3/NCN$ and alumina/NCN composites can also be confirmed by the appearance of Raman peaks around 1575 (G band) and 1350 cm^{-1} (D band) in Raman spectroscopy, as shown in Fig. 4.

Electrocatalytic evolution of hydrogen on the $NiCu/Al_2O_3/NCN$ composite electrode

Cathodic polarization curves

Cathodic polarization curves were used to evaluate the electrocatalytic activity of different composite electrodes for the HER. Figure 5 showed the polarization curves of graphite, alumina/NCN, and $NiCu/Al_2O_3/NCN$ composite electrodes in 1 M NaOH solution at ambient temperature (about 20 °C). Where, the current density was based on the geometric area of electrodes. The HER current for the electrode commenced at the onset potential of about −1.0 V at which hydrogen evolution occurred on the

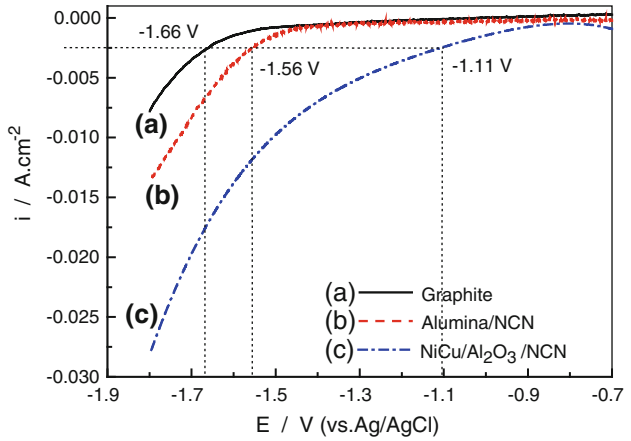

Fig. 5 Cathodic polarization curves of different electrodes in 1 M NaOH solution at 2 mVs^{-1}. Temperature: 20 °C, the geometric electrode area of electrodes: 1 cm^2, thermodynamic potential of H^+/H_2 couple: −1.01 V vs. AglAgCl at pH 14. (*a*) Graphite, (*b*) alumina/NCN, and (*c*) $NiCu/Al_2O_3/NCN$

electrode surface because some hydrogen bubbles were observed in the solution. The measured onset potential of the $NiCu/Al_2O_3/NCN$ composite electrode for HER was significantly more positive than those of the alumina/NCN electrode (about −1.4 V) and the graphite electrode (about −1.5 V). At the same HER current density (e.g., 2.5 $mAcm^{-2}$), the HER potential on $NiCu/Al_2O_3/NCN$ electrode (−1.11 V) was more positive than those of alumina/NCN (−1.56 V) and graphite (−1.66 V) electrodes. Therefore, it should be concluded that the over-potential of $NiCu/Al_2O_3/NCN$ composite electrode for hydrogen evolution was lower than those of alumina/NCN and graphite electrodes. The $NiCu/Al_2O_3/NCN$ composite electrode displayed high electrochemical activity for hydrogen evolution. Namely, by electrodepositing NiCu particles onto the surface of the conductive alumina/NCN composite material, its electrocatalytic activity for HER was improved remarkably.

The enhanced performance of electrodes toward electrocatalytic activity of HER was strongly attributed to its chemical composition and microstructure. The real surface area of the composite electrodes can be evaluated by comparison of the double layer capacitances with 20 μFcm^{-2} for pure mercury because pure mercury surface is the smoothest of all the materials and its double layer capacitive value is 20 μFcm^{-2} [27]. The double layer capacitances were determinated by analyzing EIS of the electrodes in 1 M NaOH solution under open circuit potential. The measured values of electrical double layer capacitance for the $NiCu/Al_2O_3/NCN$ composite, alumina/NCN composite and graphite electrodes were about 1.3×10^4 μFcm^{-2}, 2.4×10^4 μFcm^{-2}, and 4×10^2 μFcm^{-2}, respectively. Therefore, the estimated values of the real surface area for the $NiCu/Al_2O_3/NCN$ composite, alumina/NCN composite, and graphite electrodes were about 650, 1200, and 20 cm^2, respectively. Compared with graphite electrode, the alumina/NCN composite had higher real surface due to the presence of NCN in alumina matrix and displayed higher electrocatalytic activity by reducing the overpotential of HER [21]. The $NiCu/Al_2O_3/NCN$ composite electrode also displayed a relatively high real surface because NiCu particles could only be deposited onto the carbon layer of the composite substrate. Moreover, the deposited NiCu particles had high intrinsic electrocatalytic effect [5]. The relatively high real surface and intrinsic electrocatalytic activity gave the $NiCu/Al_2O_3/NCN$ composite electrode high electrochemical activity for HER.

In order to further illustrate the electro-oxidation activity of the $NiCu/Al_2O_3/NCN$ electrode for HER, the $Ni/Al_2O_3/NCN$ and $Cu/Al_2O_3/NCN$ composite electrodes were prepared under the same depositing conditions in 0.53 M $NiSO_4 \cdot 6H_2O$ + 0.17 M $Ni(AC)_2 \cdot 4H_2O$ + 0.26 M $Na_3C_6H_5O_7 \cdot 2H_2O$ + 0.15 M $(NH_4)_2SO_4$ solution and in 0.05 M $CuSO_4 \cdot 5H_2O$ + 0.26 M $Na_3C_6H_5O_7 \cdot 2H_2O$ + 0.15 M $(NH_4)_2SO_4$ solution, respectively. Figure 6 showed cathodic polarization curves of $NiCu/Al_2O_3/NCN$, $Ni/Al_2O_3/NCN$, and $Cu/Al_2O_3/NCN$ composite electrodes in 1 M NaOH solution. Obviously, at the same HER current density (e.g., 2.5 $mAcm^{-2}$), the HER potential on $NiCu/Al_2O_3/NCN$ electrode (−1.11 V) was more positive than those of $Ni/Al_2O_3/NCN$ (−1.23 V) and $Cu/Al_2O_3/NCN$ (−1.54 V) electrodes. The $NiCu/Al_2O_3/NCN$ composite electrode displayed the higher electrocatalytic activity for HER than the $Ni/Al_2O_3/NCN$ and $Cu/Al_2O_3/NCN$ composite electrodes. In order to try to decouple the intrinsic activity of the NiCu alloy toward hydrogen evolution from surface area increase effect, the real HER current densities

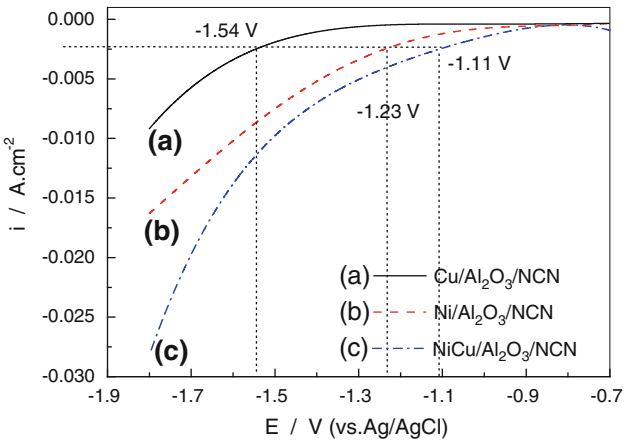

Fig. 6 Cathodic polarization curves of different electrodes in 1 M NaOH solution at 2 mVs^{-1}. Temperature: 20 °C, the geometric electrode area of electrodes: 1 cm^2, thermodynamic potential of H^+/H_2 couple: −1.01 V vs. AglAgCl at pH 14. (*a*) $Cu/Al_2O_3/NCN$, (*b*) $Ni/Al_2O_3/NCN$, and (*c*) $NiCu/Al_2O_3/NCN$

Table 1 The apparent and real HER current densities for the composite electrodes at selected potentials

Electrode materials	Real surface area (cm^2)	−1.23 V		−1.54 V	
		Apparent current density[a] (mA cm^{-2})	Real current density (mA cm^{-2})	Apparent current density[a] (mA cm^{-2})	Real current density (mA cm^{-2})
$NiCu/Al_2O_3/NCN$	650	4.0	0.006	11.2	0.017
$Ni/Al_2O_3/NCN$	295	2.4	0.008	8.6	0.029
$Cu/Al_2O_3/NCN$	285	0.3	0.001	2.5	0.009

[a] The apparent HER current density was based on the geometric area of the electrode

based on the real surface area for different composite electrodes were calculated. The real surface area was estimated by the electrical double layer capacitance from EIS results. The measured values of electrical double layer capacitance for the $NiCu/Al_2O_3/NCN$, $Ni/Al_2O_3/NCN$, and $Cu/Al_2O_3/NCN$ composites electrodes were about 1.3×10^4, 5.9×10^3, and 5.7×10^3 μFcm^{-2}, determinated by EIS measurement under open circuit potential. The estimated values of the real surface area for the $Ni/Al_2O_3/NCN$ and $Cu/Al_2O_3/NCN$ composites electrodes were about 650, 295, and 285 cm^2, respectively. Table 1 showed the real HER current densities for the three composite electrodes at selected potentials. From Table 1, it can be found that at the same HER potential, the real HER current densities based on the real surface area for the $NiCu/Al_2O_3/NCN$ and $Ni/Al_2O_3/NCN$ electrodes were obviously higher than that of $Cu/Al_2O_3/NCN$ electrode, showing that the intrinsic activity of the NiCu and Ni particles toward HER was remarkable higher than that of Cu particles. However, at the same HER potential, the real HER current densities for the $NiCu/Al_2O_3/NCN$ electrode were substantially smaller than that of $Ni/Al_2O_3/NCN$ electrode. This, to some extent, showed that the intrinsic activity of the $NiCu/Al_2O_3/NCN$ electrode toward HER was not higher than that of the $Ni/Al_2O_3/NCN$ electrode and modification of nickel by copper did not enhance its intrinsic electro-catalytic activity for HER. This seemed to suggest the improved electrocatalytic activity of $NiCu/Al_2O_3/NCN$ electrode for HER was mainly due to the increased surface area effect but not the synergistic effect of the Ni and Cu. However, Solmaz et al. [5, 21] found that the HER activity of the Cu/NiCu electrode was higher than the Cu and Cu/Ni electrodes in their study of the characterization of NiCu coatings as cathode materials for HER, and pointed out that the catalytic activity of the NiCu coating was related to the porosity as well as synergistic effect of the Ni and Cu. Therefore, this research on intrinsic activity of the NiCu alloy or particles was needed further later. Nevertheless, it was undoubted that the $NiCu/Al_2O_3/NCN$ electrode presented the higher electrochemical activity in alkaline medium for HER due to the presence of NiCu particles on the electrode surface.

EIS

Figure 7 showed EIS spectra of the graphite, alumina/NCN composite, and $NiCu/Al_2O_3/NCN$ composite electrodes in 1 M NaOH solution at a HER overpotential of 300 mV. Figure 8 showed EIS spectra of the $NiCu/Al_2O_3/NCN$ composite electrode in 1 M NaOH solution at different HER overpotentials. From Fig. 7, it can be seen that the impedance spectra for the alumina/NCN and $NiCu/Al_2O_3/NCN$ composite electrodes under investigation displayed two obviously depressed semicircles in the complex plane plots ($-Z_{im}$ vs. Z_{re}) and the semicircles in the high frequency (HF) region were almost the same in size. Moreover, for the $NiCu/Al_2O_3/NCN$ (shown in Fig. 8) and alumina/NCN (not shown) composite electrode, the HF semicircle was almost independent of the HER overpotentials. As the potential affect the kinetics of the reaction, it can be concluded that the HF semicircle was not related to the electrode kinetics and was attributed to the low-conductivity continuous phase (alumina) [27, 30].

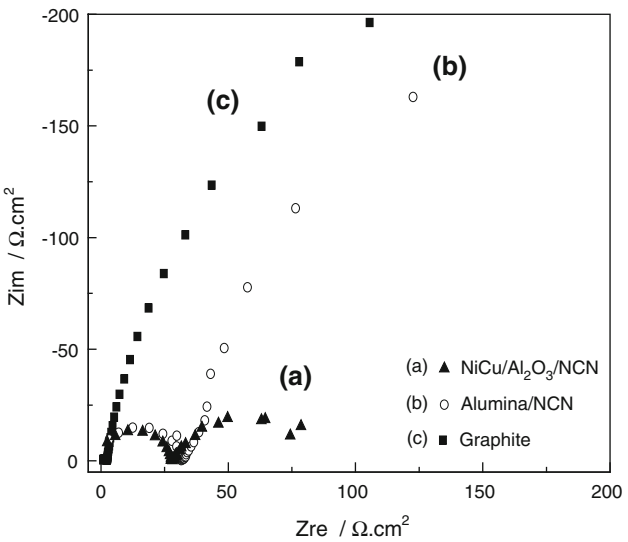

Fig. 7 EIS of the (*a*) $NiCu/Al_2O_3/NCN$ composite, (*b*) alumina/NCN, and (*c*) graphite electrodes in 1 M NaOH at a HER overpotential of 300 mV

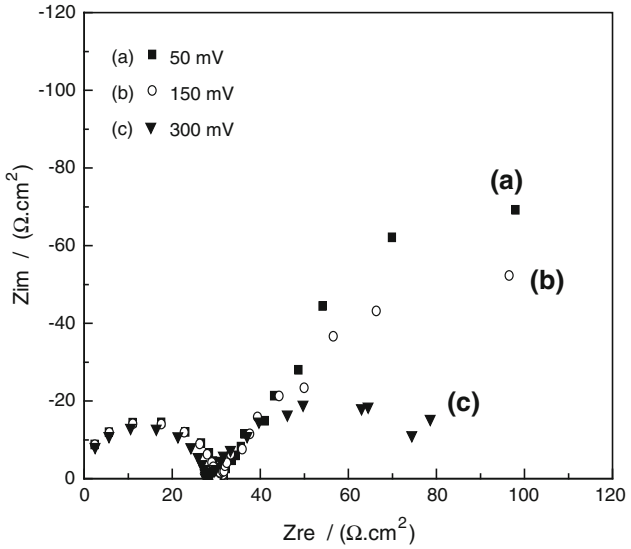

Fig. 8 EIS of the $NiCu/Al_2O_3/NCN$ composite electrode in 1 M NaOH at different additional overpotentials: (*a*) 50 mV, (*b*) 150 mV, and (*c*) 300 mV

From Fig. 8, we can also find that the semicircle in the low frequency (LF) region varied with the overpotentials, which was attributed to the charge transfer resistance (R_{ct}) of the HER [27, 30]. The similar change went for the alumina/NCN and graphite electrodes (not shown). Therefore, the R_{ct} for the HER was approximated from this LF semicircle. When the potentials applied to the electrode increased, the R_{ct} decreased correspondingly. Since only one LF semicircle was involved in hydrogen evolution in the impedance plane plots, the HER on the electrode should be simple hydrogen evolution processes [27, 30]. Some authors [5, 13, 16, 31] verified in their study that the overall hydrogen evolution for graphite composite-coated electrode, nickel–Mo powder composite, Ni nano-wires as well as NiCu alloy electrode was controlled by electrochemical process in an alkaline. Therefore, the charge transfer resistance (R_{ct}) can, to some extent, represents the electrocatalytic activity toward HER in this case. The values of charge transfer resistance (R_{ct}) for electrodes, determinated by EIS measurements in 1 M NaOH at the overpotential of 300 mV, are shown in Table 2. The exchange current density i^0 is summarized in Table 2, which was determined by the extrapolating over-potential (η) against $-\lg R_{ct}$ according to following expression [32, 33].

$$\eta = -\frac{2.3}{\alpha f}\lg(\alpha f i^0) - \frac{2.3}{\alpha f}\lg R_{ct}, \quad (1)$$

where, α is the energy-transfer coefficient and $f = \frac{F}{RT}$.

A comparison among these kinetic parameters revealed that the $NiCu/Al_2O_3/NCN$ composite electrode had remarkably enhanced its reaction activity for HER. The lower charge transfer resistance (R_{ct}) as well as higher value of the estimated exchange current density (i^0) gave the $NiCu/Al_2O_3/NCN$ composite electrode higher electrocatalytic activity for HER than those of the graphite and the alumina/NCN composite electrodes in this study.

Table 2 HER kinetic parameters for the alumina/NCN and $NiCu/Al_2O_3/NCN$ composite electrodes

Electrode materials	R_{ct} (Ωcm^2)	i^0 (μAcm^{-2})
$NiCu/Al_2O_3/NCN$	59.5	280
$Ni/Al_2O_3/NCN$	45.4	68
Alumina/NCN	1177	15
Graphite	1246	10 [29]

Based on above experimental results, to further discuss its practical potential, the electrocatalytic activity of the $NiCu/Al_2O_3/NCN$ composite electrode was compared to traditional electrolysis cathodes such as Ni and Raney-Ni cathodes according to Tanaka's study [34]. The HER current density (about 4 $mAcm^{-2}$ at -1.23 V) and exchange current density i^0 (about 280 μAcm^{-2}) on the $NiCu/Al_2O_3/NCN$ composite electrode were obviously lower than those of Raney-Ni electrode (about 200 $mAcm^{-2}$ at -1.23 V, $i^0 = 4450$ μAcm^{-2}), but higher than those of Ni electrode (about 3 $mAcm^{-2}$ at -1.23 V, $i^0 = 10.9$ μAcm^{-2}). This indicated the electrocatalytic activity of the $NiCu/Al_2O_3/NCN$ composite electrode was lower than that of Raney-Ni cathode but higher than that of Ni electrode. However, considering its very low loadings of active particles, the $NiCu/Al_2O_3/NCN$ composite electrodes still showed a high sensibility for HER. This result indicated that the Al_2O_3/NCN composite still had a potential as the catalyst support.

Potentiostatic curves

Physical, chemical, and electrochemical stability of electrode material was one of the important characteristics that must be established. Thus, the composite electrode was tested through long term working experiments by operating at a constant applied potential of -1400 mV at 298 K in 1 M NaOH, and its current response (chronoamperogram) was recorded (Fig. 9). As can be seen, under the same potential applied, the measured current on the $NiCu/Al_2O_3/NCN$ composite electrode was higher and more stable than those on $Ni/Al_2O_3/NCN$ and Al_2O_3/NCN composite electrodes. This indicated that the activities of the $NiCu/Al_2O_3/NCN$ composite electrode were higher than those of the $Ni/Al_2O_3/NCN$ and Al_2O_3/NCN composite electrodes. From the highest to the lowest, the order of their HER activities was: $NiCu/Al_2O_3/NCN > Ni/Al_2O_3/NCN > Al_2O_3/NCN$.

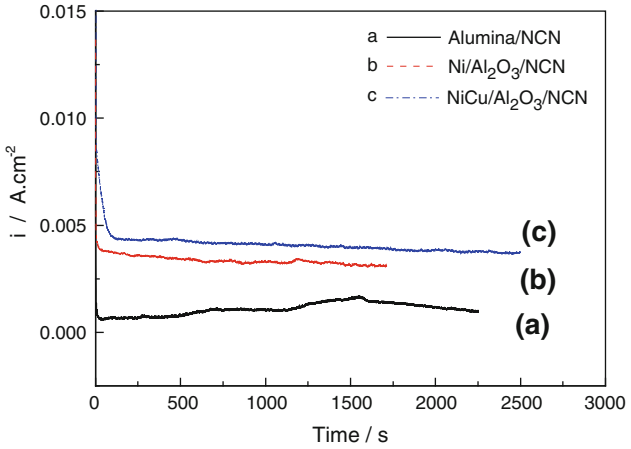

Fig. 9 Current–time curves of (*a*) alumina/NCN, (*b*) $Ni/Al_2O_3/NCN$, and (*c*) $NiCu/Al_2O_3/NCN$ composite electrodes at −1400 mV (vs. Ag/AgCl-saturated KCl)

Conclusion

We have fabricated the $NiCu/Al_2O_3/NCN$ composite electrode by coelectrodepositing Ni–Cu particles, using a novel conductive alumina/NCN composite material as the support. Nickel–copper particles were briefly deposited and uniformly distributed over the carbon layer of the conductive ceramics between alumina grains, in the form of a NiCu solid solution with fcc structure. The $NiCu/Al_2O_3/NCN$ composite displayed high electrochemical stability in alkaline solution and relatively high electrocatalytic activity for HER due to its relatively high real surface area and high intrinsic electrocatalytic effect of NiCu particles.

References

1. Vezirolu TN, Barbir F (1992) Int J Hydrogen Energy 17:391
2. Abanades S, Legal A, Cordier A, Peraudeau G, Flamant G, Julbe A (2010) J Mater Sci 45:4163. doi:10.1007/s10853-010-4506-4
3. Hu MZ, Lai P, Bhuiyan MS, Tsouris C, Gu B, Paranthaman MP, Gabitto J, Harrison L (2009) J Mater Sci 44:2820. doi:10.1007/s10853-009-3372-4
4. El-Deab MS, Saleh MM (2003) Int J Hydrogen Energy 28:1199
5. Solmaz R, Doner A, Kardas G (2008) Electrochem Commun 10:1909
6. Xu W, Liu C, Xing W, Lu T (2007) Electrochem Commun 9:180
7. Marshall AT, Sunde S, Tsypkin M, Tunold R (2007) Int J Hydrogen Energy 32:2320
8. Stojic DL, Grozdic TD, Kaninski MPM, Stanic V (2007) Int J Hydrogen Energy 32:2314
9. Han Q, Liu K, Chen J, Wei X (2009) Int J Hydrogen Energy 34:71
10. Xu Y (2009) Int J Hydrogen Energy 34:77
11. Crnkovic FC, Machado SAS, Avaca LA (2004) Int J Hydrogen Energy 29:249
12. Burchardt T (2000) Int J Hydrogen Energy 25:627
13. Lee JK, Yi Y, Lee HJ, Uhm S, Lee J (2009) Catal Today 146:188
14. Han Q, Liu K, Chen J, Wei X (2003) Int J Hydrogen Energy 28:1207
15. Shibli SMA, Dilimon VS (2007) Int J Hydrogen Energy 32:1694
16. Kubisztal J, Budniok A, Lasia A (2007) Int J Hydrogen Energy 32:1211
17. Alisa NF, Sasha O (2005) J Mol Catal A Chem 242:182
18. Kibria MF, Mridha MSH (1996) Int J Hydrogen Energy 21:179
19. Kellenberger A, Vaszilcsin N, Brandl W, Duteanu N (2007) Int J Hydrogen Energy 32:3258
20. Kim DR, Cho KW, Choi YI, Park CJ (2009) Int J Hydrogen Energy 34:2622
21. Solmaz R, Doner A, Kardas G (2009) Int J Hydrogen Energy 34:2089
22. Menchavez RL, Fuji M, Takahashi M (2008) Adv Mater 20:2345
23. Menchavez RL, Fuji M, Takahashi M (2009) J Eur Ceram Soc 29:949
24. Hai C, Liu J, Watanabe H, Fuji M, Wang F, Takahashi M (2009) J Am Ceram Soc 92:s38
25. Liu J, Menchavez RL, Watanabe H, Fuji M, Takahashi M (2008) Electrochim Acta 53:7191
26. Metikos-Hukovic M, Jukic A (2000) Electrochim Acta 45:4159
27. Liu J, Watanabe H, Fuji M, Takahashi M (2009) Electrochem Commun 11:107
28. Alper M, Kockar H, Safak M, Celalettin Baykul M (2008) J Alloy Compd 453:15
29. Danaee I, Jafarian M, Forouzandeh F, Gobal F, Mahjani MG (2009) Int J Hydrogen Energy 34:859
30. Shervedani RK, Madram AR (2007) Electrochim Acta 53:426
31. Dabo P, Menard H, Brossard L (1997) Int J Hydrogen Energy 22:763
32. Ma J, Jiang X (1995) Chin J Appl Chem 12(6):25
33. Elumalai P, Vasan HN, Munichandraiah N, Shivashankar SA (2002) J Appl Electrochem 32:1005
34. Tanaka S, Hirose N, Tanaki T, Ogata YH (2001) Int J Hydrogen Energy 26:47